Materials Views
www.MaterialsViews.com

ADVANCED FUNCTIONAL MATERIALS
www.afm-journal.de

FULL PAPER

Controlling Surface Plasmon Optical Transmission with an Electrochemical Switch Using Conducting Polymer Thin Films

Akira Baba, Kohji Tada, Rapiphun Janmanee, Saengrawee Sriwichai, Kazunari Shinbo, Keizo Kato, Futao Kaneko, and Sukon Phanichphant*

Surface plasmon resonance (SPR)-enhanced optical transmission is actively controlled by an electrochromism of conducting polymer thin films. Polyaniline and poly(3,4-ethylenedioxythiophene) thin films are deposited on a thin gold grating surface. SPR-enhanced optical transmission is demonstrated by irradiating white light on the conducting polymer thin film–gold grating surface and detecting the transmitted light from the back side. The transmission SPR system is combined with an electrochemical setup to manipulate the resonance. The wavelength of the sharp peak in the transmission light spectra is tuned by electrochemical doping/dedoping of the conducting polymer thin films. The present study of controllable SPR-enhanced optical transmission should provide novel active plasmonic devices such as active bandpass filters or biosensors.

1. Introduction

Surface plasmon resonance (SPR) phenomena have attracted considerable attention since many years because of the extremely strong enhancement and confinement of electric fields near metal surfaces.[1] This leads to sensitive detection of small changes in surface environments, which allows for determination of optical constants and the thickness of layered systems. A combination of SPR and electrochemical measurements has been demonstrated as a powerful technique for simultaneous characterization and manipulation of electrode–electrolyte interfaces.[2–4] Recently, the electrochemical SPR technique was applied for the characterization of conducting polymer thin films.[5–8] This involves in situ monitoring of the film swelling/contraction and electrochromic properties during electropolymerization or the anion doping/dedoping process of deposited conducting polymers. The change in the doping state allows one to tune the SPR conditions with a prism coupling-attenuated total reflection mode in the Kretschmann configuration.[9]

Recently, active plasmonic devices such as filters and modulators have become a hot topic in the field of SPR-enhanced optical field. In these studies, metal nanoparticles or metal nanoarrays are used to excite localized SPR, which produces a surface plasmon absorption band in the visible region. These active plasmonic devices are based on controlling light trapping or light absorption at the surface of metals as a result of surface plasmon excitation, which can be tuned using liquid crystals,[10,11] electroactive conducting polymers,[12] and photochromic polymers[13] on metal arrays.

As another effect, surface plasmon excitation has recently been shown to enhance light transmission through nanostructures such as hole arrays and grating patterns[14,15] and, of particular interest, through grating substrates of commercial digital versatile disc-recordables (DVD-Rs) coated with thin gold films.[16,17] Optical transmission is based on the decoupling of surface plasmons that are excited and confined at the surface of metals. Hence, the transmission SPR (T-SPR) spectrum is highly sensitive to the local refractive index near a metal–dielectric interface, making T-SPR spectroscopy a useful technique for optical sensing applications.

In this study, we present actively tuned SPR-enhanced transmission with conducting polymer thin films. Polyaniline (PANI) and poly(3,4-ethylenedioxythiophene) (PEDOT) thin films were deposited on a thin gold grating surface by electropolymerization. We used these two polymers because they showed the large change of wavelength dependent complex dielectric constants by controlling the potential. DVD-R substrates were used either directly as grating substrates or templates for grating substrate imprinting. The use of grating surfaces on commercially available CD-Rs, DVD-Rs, and BD-Rs is a convenient method of obtaining the grating-coupled SPRs.[18–21] A T-SPR system was combined with an electrochemical setup to manipulate the resonance. SPR-enhanced optical transmission was obtained by the irradiation of white light on the conducting

Prof. A. Baba, K. Tada, R. Janmanee, Prof. K. Shinbo,
Prof. K. Kato, Prof. F. Kaneko
Center for Transdisciplinary Research
and Graduate School of Science and Technology
Niigata University
8050 Ikarashi 2-nocho, Nishi-ku, Niigata 950-2181, Japan
E-mail: ababa@eng.niigata-u.ac.jp
Dr. S. Sriwichai, Prof. S. Phanichphant
Department of Chemistry and Center for Innovation in Chemistry
Faculty of Science
Chiang Mai University
Chiang Mai 50200, Thailand

DOI: 10.1002/adfm.201200373

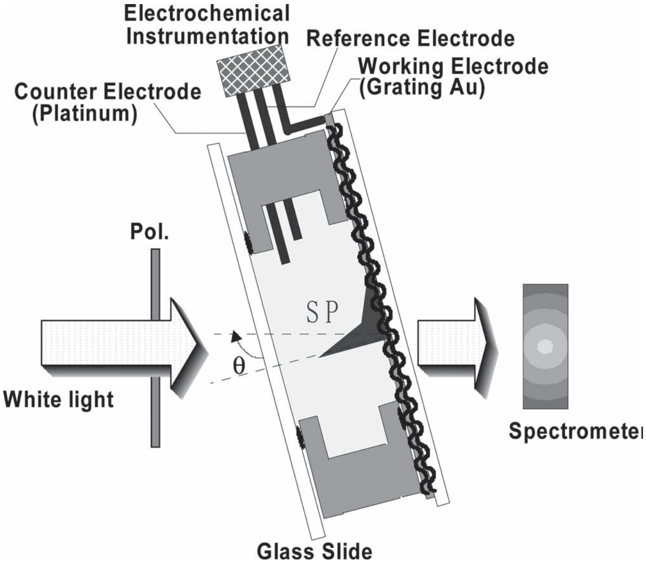

Figure 1. Schematic of the electrochemically controlled transmission surface plasmon resonance setup (grating pitch, $\Lambda = 740$ nm, grating height ≈ 130 nm, tickness of gold ≈ 130 nm).

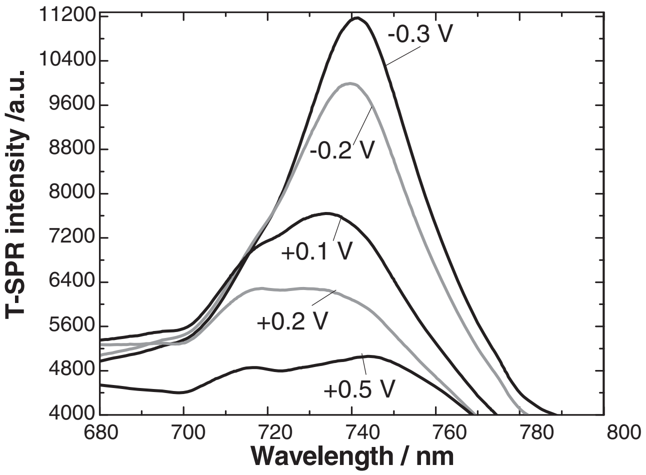

Figure 2. T-SPR spectra of PANI thin film on gold grating substrate in aqueous H_2SO_4 for various constant potentials (–0.3, –0.2, +0.1, +0.2 and +0.5 V) at a light incident angle of 35°.

polymer thin film–gold grating surface and detected from the back side as shown in **Figure 1**. The intensity or wavelength of the sharp peak in the transmission light spectra was actively tuned by electrochemical doping/dedoping of the conducting polymer thin films. Our method allows enhanced transmission of selected wavelengths whereas absorption-based methods work on the principle of reduced transmission of selected wavelengths. Furthermore, to understand the experimental results, finite-difference time-domain (FDTD) simulations were performed by assuming the device structures with grating. The present study of controllable SPR-enhanced optical transmission should provide novel active plasmonic devices such as active band pass filters or biosensors.

2. Results and Discussion

2.1. Tuning of T-SPR Properties as a Function of Wavelength

First, the electropolymerized PANI thin film was used as an electroactive conducting polymer material because the film showed large electrochromism in the visible region. The PANI film was deposited on the gold grating substrates by cycling the potential between –0.2 and 0.9 V at a scan rate of 20 mV/s for 10 cycles. Based on our previous report, the thickness of the deposited film was estimated to be 50 nm.[9]

Figure 2 shows T-SPR spectra of the PANI thin film on the gold grating substrate in aqueous H_2SO_4 at constant potentials (from –0.3 to +0.5 V) at a light incident angle of 35°. We chose the incident angle at which the transmission peak due to the surface plasmon excitation was clearly observed.The PANI film became fully dedoped (leucoemeraldine) at –0.3 V and changed to a fully doped state (emeraldine) at +0.5 V. A sharp T-SPR peak was observed at –0.3 V, which was then electrochemically controlled by switching the potential. By gradually changing the doping level, the T-SPR peak gradually decreased and completely quenched at the doped state of +0.5 V. T-SPR peak switching could be observed repeatedly. As previously reported, the electron transfer from the electrodeposited PANI film to the electrode occurred by applying the potential. To compensate for the charge of the PANI film, anion transport from the electrolyte solution (i.e., anion doping)[22,23] should occur. This phenomenon is responsible for the dramatic change in the complex dielectric constant of the PANI film. It is known that the switching time between the doped and dedoped states for electropolymerized PANI is in the range of microseconds, and the doped/dedoped process can be cycled by more than 10^5 times without degradation.[24] Because the doped PANI film has strong absorption in the observed wavelength range between 680 and 800 nm,[25] the quenched T-SPR peak should occur primarily because of changes in the imaginary part of the dielectric constant. The results show that the on/off tuning of the SPR-enhanced transmission light can be electrochemically achieved with the PANI thin film.

Next, we used the PEDOT thin film instead of the PANI film. PEDOT is also known to exhibit a high contrast in the visible region upon electrochromic switching. The thickness of the deposited film is ≈30 nm. By switching from the dedoped to the doped state, a significant color change occurs from dark blue to transparent sky blue.[26,27] **Figure 3**a shows the T-SPR spectra of the PEDOT thin film on the gold grating substrate in the acetonitrile solution with 0.1 M tetrabutylammonium hexafluorophosphate ($TBAPF_6$) at each constant potential (–1.0, –0.65, –0.2, and +0.5 V) at a light incident angle of 0°. The sharp peak at 723 nm was observed at the dedoped state of –1.0 V. At –0.65 V, the peak shifted to a shorter wavelength and became broader. By doping at +0.5 V, the peak shifted further to a shorter wavelength at 578 nm, and the strong transmission with a sharp peak was again observed. It is noticeable that a significant change, more than a 150-nm peak wavelength shift, can be obtained with the electrochemically controlled PEDOT thin

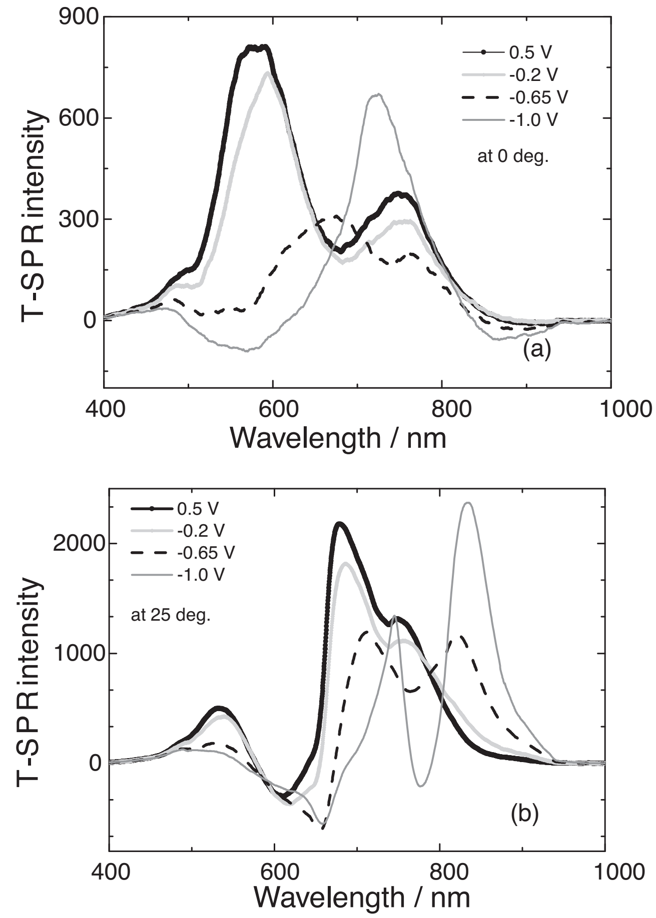

Figure 3. Tuning of T-SPR spectra of PEDOT thin film on gold grating substrate in acetnitrile solution with 0.1 M $TBAPF_6$ for various constant potentials (–1.0, –0.65, –0.2, and +0.5 V) at the light incident angles of 0° (a) and 25° (b).

film. Compared with the intensity tuning with the PANI film, this result indicates that wavelength tuning is also possible with the PEDOT thin film. The different behavior between the PANI and PEDOT is due to the different wavelength dependence of dielectric constants at each potential. These results correspod with the tuning of SPR excitation using prism-coupling technique[9] and absorption based LSPR observation.[12] Although slight thickness changes due to doping/dedoping of the PEDOT film might occur, a large change in the peak wavelength may be responsible for the change in the complex dielectric constants in the visible region, because the wavelength of the T-SPR peak mainly depends on both real and imaginary parts of the dielectric constant of adsorbed materials on the metal grating. It should be noted that the imaginary part of the dielectric constant corresponds to the extinction coefficient at the probe wavelength. However, because the electrochemical tuning of the T-SPR peak of PEDOT does not exhibit changes similar to those of dielectic functions,[9] the change in T-SPR occurs owing to the change in the surface plasmon excitation wavelength due to the change in the real part of the PEDOT film dielectric constant. This is because the surface plasmon dispersion is changed by the change of real part of dielectric constant of the deposited film on the gold grating surface. Reverse changes in the wavelength were also observed repeatedly. This demonstrates that the PEDOT thin film can easily tune the plasmon resonance on the grating surface. When the incident angle is changed to 25°, each peak wavelength red-shifts (about 100 nm) at all doping states (e.g., the peak wavelength 578 nm at the incident angle 0° shifts to 679 nm at 25° at +0.5 V). It is interesting to note that the peak wavelength can be also tuned by rotating the sample, which gives a wide range of tuning (>250 nm) for the peak wavelength (e.g., the peak wavelength can be changed from 578 nm at 0.5 V at 0° to 833 nm at –1 V at 25°).

2.2. Tuning of T-SPR Intensity by Cyclic Voltammetry at Fixed Wavelengths

Then, in situ reversible tuning of T-SPR was obtained by cycling the potential between –1.0 and 0.5 V at a scan rate of 20 mV/s. The T-SPR intensity was monitored at wavelengths slightly lower than the maximum peak wavelengths at incident angles of 0° and 25° as shown in **Figure 4**. In the anodic scan of the incident angle of 0°, the T-SPR intensity sharply increased from –1.0 to –0.1 V. This value corresponds to the oxidation peak in the constant voltage. The T-SPR intensity change can be explained by the change in the dielectric constant due to the doping of the PEDOT thin film. The T-SPR intensity almost plateaued above –0.1 V. This suggests that the dielectric constant of the PEDOT thin film is almost constant above this potential. In the cathodic scan, the onset of the reflectivity change was observed at –0.1 V. In case of the incident angle of 25°, the trend of the T-SPR intensity change during the potential cycling was opposite to that of 0°, and the curve was also almost constant above –0.1 V. It should be noted that the transmitted light intensity change without surface plasmon excitation (s-pol) is much smaller than that with surface plasmon excitation (p-pol, see Supporting Information). This clearly indicates that the decoupling of surface plasmon at the back side contributes to the enhancement of transmission of the light.

2.3. Tuning of T-SPR Intensity at Constant Potentials

To further explore the T-SPR tuning properties, the response of the T-SPR intensity to the application of a sequence of potential steps was studied as shown in **Figure 5**. The potential was switched sequentially between the doped and the dedoped states, i.e., applied in the following sequence: +0.5 → –0.2 → –0.65 → –1.0 → 0.5 V. Each potential was applied for 60 s. At 550 nm at 0°, the T-SPR intensity decreased stepwise when the PEDOT film was dedoped, and it shifted back to the initial intensity at the doped state when 0.5 V was again applied. In contrast, the T-SPR intensity increased stepwise upon dedoping at 825 nm at the incident angle of 25° (reverse behavior). This phenomenon is extremely useful in designing optical switching devices because one can obtain different T-SPR tuning by controlling the wavelength and incident angle. This switching property is in accordance with the result obtained from the T-SPR spectra as a function of wavelength as shown in Figure 3. The T-SPR intensity changed almost immediately when the potential step

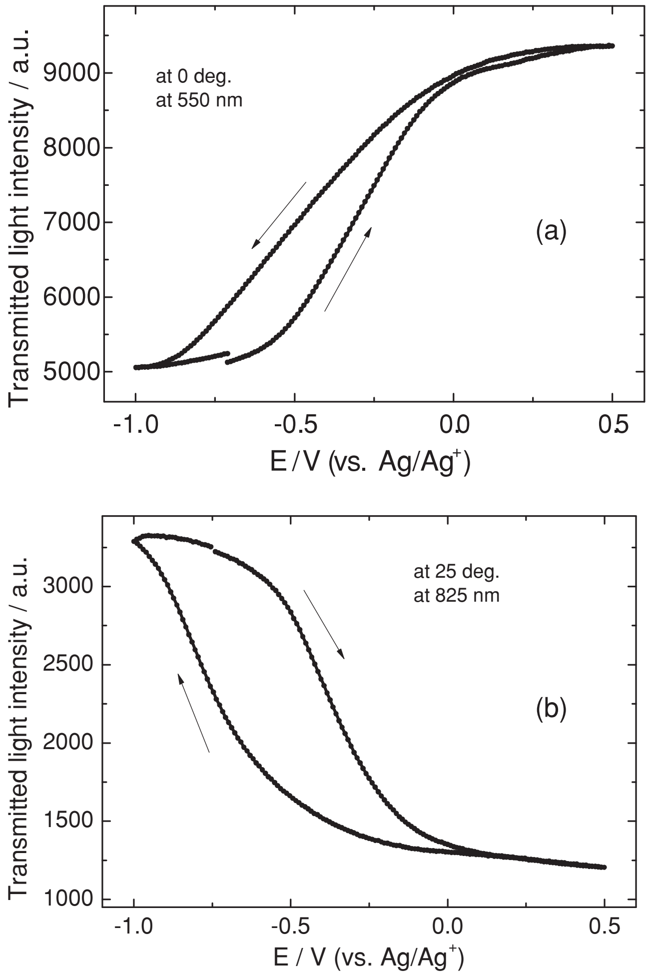

Figure 4. In situ reversible tuning of T-SPR obtained by cycling the potential between –1.0 and 0.5 V at a scan rate of 20 mV/s at light incident angles of 0° (a) and 25° (b).

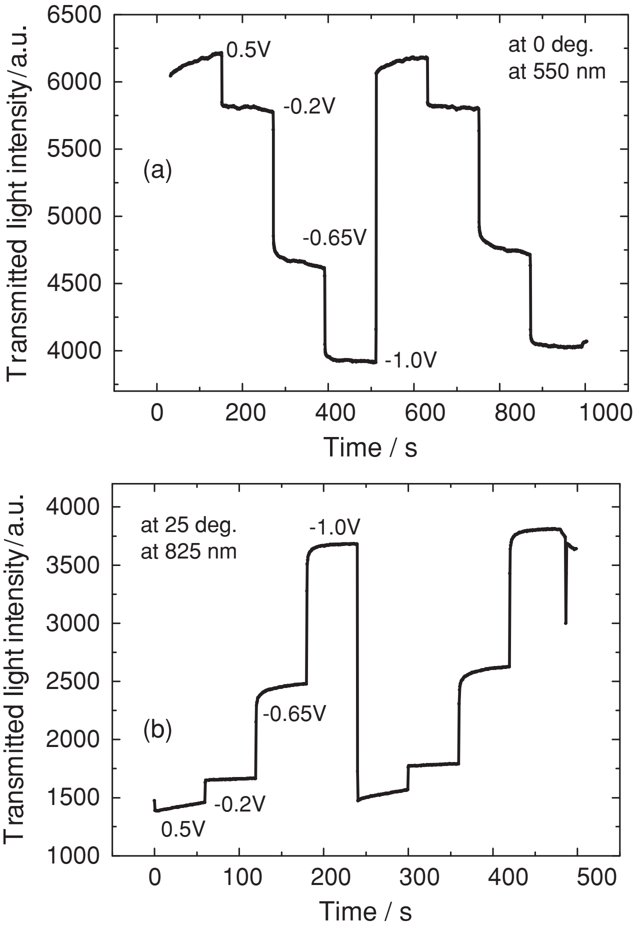

Figure 5. Response of the T-SPR intensity to a sequence of applied potential steps at 550 nm at the incident angle of 0° (a) and at 825 nm at the incident angle of 25° (b).

was applied, and it reached a plateau for each potential applied. The slight change at 0.5 and –0.65 V occurs probably because of the film swelling/shrinking by anion doping/dedoping.

2.4. FDTD Simulations

To study the origin of the transmission enhancement with conducting polymers, we simulated the electric field of the device using the FDTD method (FDTD solutions). **Figure 6** shows the electric field intensity maps of electrolyte–PEDOT films (30 nm) with a gold (thickness 50 nm) polycarbonate grating structure (grating pitch, $\Lambda = 740$ nm) upon irradiation with p-polarized light at a wavelength of 590 nm at an incident angle of 0° (a,b) and at a wavelength of 825 nm at an incident angle of 25° (c,d). Fully doped state at 0.5 V (a,c) and dedoped state at –1.0 V (b,d) are assumed. The color bar shows the electric field intensity. The assumed structure is also shown in the figure. In the simulation, the dielectric constants of PEDOT films at each doping state were obtained from our previous reports ($\varepsilon' + \varepsilon'' = 1.79 + i0.1$ in the doped state and $\varepsilon' + \varepsilon'' = 1.8 + i0.85$ in the dedoped state at a wavelength of ≈590 nm, and $\varepsilon' + \varepsilon'' = 1.68 + i0.29$ in the doped state and $\varepsilon' + \varepsilon'' = 2.28 + i0.11$ in the dedoped state at a wavelength of ≈825 nm).[9b] As shown in Figure 6a (at doped state at 590 nm), a strongly enhanced electric field was observed near the Au grating surface, indicating the excitation of the surface plasmons. It should be noted that light is transferred through the continuous thin gold grating film (thickness 50 nm) as seen in the near field on the polycarbonate side, which is similar to the phenomena observed with metal nanoholes[14] or thick metal grating with small slits.[16] Furthermore, the electric field intensity on Au grating surface obviously decreased when the PEDOT film switched to the dedoped state (Figure 6b). This indicates that the electric field on the Au surface can be controlled by the doping state of the thin PEDOT film. In contrast, in the case of 825 nm at an incident angle of 25°, which corresponds to another T-SPR peak observed in Figure 3, the electric field intensity near the Au grating at dedoped state is stronger than that at doped state. These FDTD results well support the experimental results that the T-SPR can be controlled systematically by the change of doping state of PEDOT film on Au suraface.

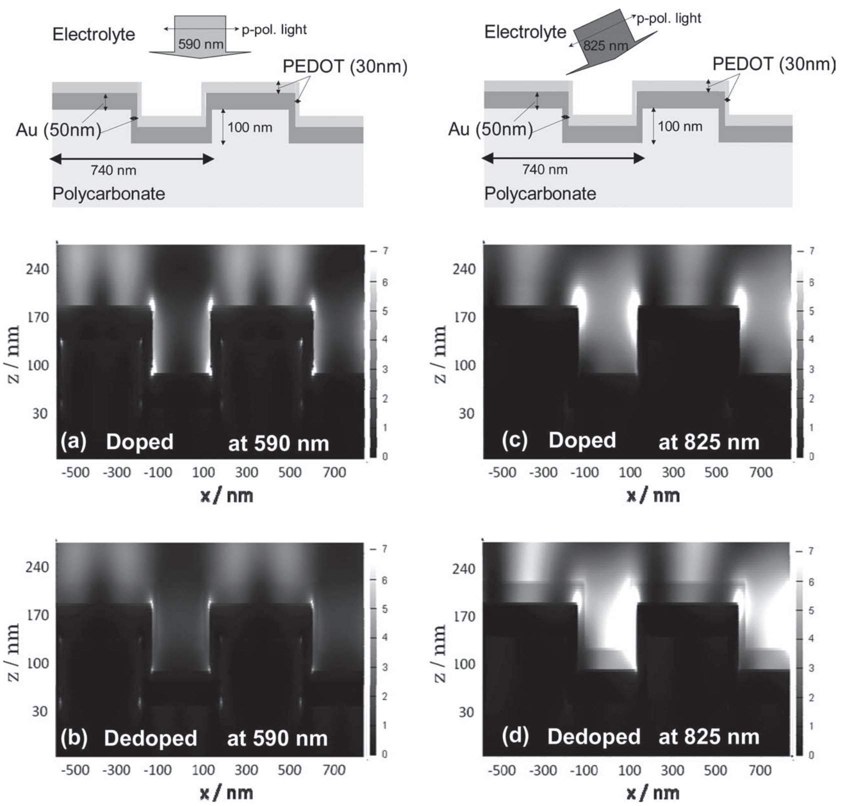

Figure 6. Electric field intensity maps of electrolyte–PEDOT films (30 nm) with a gold (thickness 50 nm) polycarbonate grating structure (grating pitch, $\Lambda = 740$ nm) upon irradiation with p-polarized light at a wavelength of 590 nm at an incident angle of 0° (a,b) and at a wavelength of 825 nm at an incident angle of 25° (c,d). Fully doped state (a,c) and dedoped state (b,d). The color bar shows electric field intensity. p-polarized plane wave irradiated from the electrolyte side is used in the simulation. The structure and parameters are shown in the schematics.

3. Conclusions

We developed a novel method of tuning and controlling SPR-enhanced transmission light by using electrochemically controlled conducting polymers. SPR-enhanced optical transmission was obtained by irradiation of white light on the conducting polymer thin film–gold grating surface. The intensity or wavelength of the sharp transmission light spectra was actively tuned by electrochemical doping/dedoping of the conducting polymer thin films. The PANI thin film showed on/off switching of the T-SPR spectra, while the PEDOT thin film exhibited wavelength tuning. The FDTD simulations showed that the electric field on the Au surface was controllable by the doping state of the thin PEDOT film on the electrolyte side. Compared with other approaches that have been demonstrated to be effective with absorption-based active plasmonic devices, our method transmits controllable SPR-enhanced transmission light through the devices, with active selection of both the wavelength and the intensity. Therefore, the demonstrated method opens new opportunities both for basic studies of the tunability of SPR-enhanced transmission of light and active plasmonic device applications using electrochemically controlled conducting polymers.

4. Experimental Section

The chemical compounds 3,4-ethylenedioxythiophene (EDOT), aniline, and tetrabutylammonium hexafluorophosphate ($TBAPF_6$) were purchased from Aldrich and used as received.

A polycarbonate DVD-R (Taiyo Yuden Co., Ltd.) was used as the diffraction grating substrate. The DVD-R was cut into pieces, which were then immersed in nitric acid to remove the dye layer on the grating side. The grating height was adjusted to ≈130 nm with a grating period of 740 nm by immersing into an etching solution comprising ethanol and acetone (4:1) for 15 min. The cleaned pieces were coated with a layer of gold (thickness ≈ 50 nm) by vacuum evaporation. In case of electrochemical measurements in an organic solvent, imprinted grating substrates were fabricated from thiolene resins (Norland Optical Adhesive, NOA81)[28] as follows: Thiolene resins were dropcasted on a DVD-R grating template, which was then pressed on a glass slide. After thiolene was cured by UV irradiation, glass-slide-thiolene was detached from the template. The grating height of the imprinted thiolene substrates was ≈100 nm.

Electrochemical T-SPR measurements were conducted with a homemade system equipped with a fiber optic spectrometer (HR 4000, Ocean Optics, Inc.) and a white light source (LS-1 tungsten halogen, Ocean Optics, Inc.). The Au grating substrates were clamped against a Teflon cell with an O-ring providing a liquid-tight seal. Then, the substrates were mounted on a rotation stage. White light was passed through a linear polarizer, and the T-SPR signals of the gold grating substrates were then detected by fiber optic spectrometry. In all measurements, only zero-order transmission was detected. Surface plasmons were excited at the metal grating–dielectric interface upon irradiation of white light at fixed incident angles. A normalized spectrum was obtained by subtracting the raw spectrum of s-polarized light from that of p-polarized light.

All potentiostatic and cyclic voltammetry measurements were performed using a one-compartment three-electrode cell driven by an HZ-5000 potentiostat (Hokuto Denko Ltd., Japan). In all measurements, the working electrodes consisted of gold films (d ≈ 50 nm), which had been vacuum-evaporated onto a glass substrate (i.e., a 2-nm Cr adhesion layer was previously evaporated onto the glass substrate). The counter electrode was a platinum wire and the reference electrode was an Ag/Ag^+ nonaqueous or an Ag/AgCl aqueous electrode. The surface area of the gold electrode was 3.14 cm^2. EDOT was electropolymerized at a constant potential by using 0.01 M EDOT monomer in an acetnitrile solution with 0.1 M $TBAPF_6$. Electrochemical measurements of PEDOT in a monomer-free solution were performed in the acetnitrile solution with 0.1 M $TBAPF_6$. Electropolymerization of aniline was achieved by applying potential cycling between –0.2 and 0.9 V at a scan rate of 20 mV/s in a 0.5 M H_2SO_4 solution containing 0.02 M aniline monomer. Electrochemical measurements of PANI in monomer-free solution were performed in a 0.5 M H_2SO_4 solution.

Supporting Information

Supporting Information is available from the Wiley Online Library or from the author.

Acknowledgements

This work was partly supported by a Grant-in-Aid for Scientific Research for Young Scientists (B) from the Japan Society for the Promotion of Science and an Adaptable and Seamless Technology transfer Program (A-STEP) from the Japan Science and Technology Agency (JST).

Received: February 7, 2012
Revised: April 27, 2012
Published online: June 18, 2012

---

[1] W. Knoll, *Annu. Rev. Phys. Chem.* **1998**, *49*, 569.
[2] A. Tadjeddine, D. M. Kolb, R. Kötz, *Surf. Sci.* **1980**, *101*, 277.
[3] J. G. Gordon II, S. Ernst, *Surf. Sci.* **1980**, *101*, 499.
[4] Y. Iwasaki, T. Horiuchi, M. Morita, O. Niwa, *Electroanalysis* **1997**, *9*, 1239.
[5] a) A. Baba, R. C. Advincula, W. Knoll, *J. Phys. Chem. B* **2002**, *106*, 1581; b) A. Baba, M. K. Park, R. C. Advincula, W. Knoll, *Langmuir* **2002**, *18*, 4648; c) A. Baba, W. Knoll. *Adv. Mater.* **2003**, *15*, 1015.
[6] V. Chegel, O. Raitman, E. Katz, R. Gabai, I. Willner, *Chem. Commun.* **2001**, 883.
[7] O. Raitman, E. Katz, I. Willner, V. Chegel, G. Popova, *Angew. Chem. Int. Ed.* **2001**, *40*, 3649.
[8] X. Kang, Y. Jin, G. Chen, S. Dong, *Langmuir* **2002**, *18*, 1713.
[9] a) A. Baba, S. J. Tian, F. Stefani, C. Xia, Z. Wang, R. C. Advincula, D. Johannsmann, W. Knoll, *J. Electroanal. Chem.* **2004**, *562*, 95; b) A. Baba, J. Lübben, K. Tamada, W. Knoll, *Langmuir* **2003**, *19*, 9058; c) A. Baba, R. Ponnapati, P. Taranekar, W. Knoll, R. Advincula, *ACS Appl. Mater. Interfaces* **2010**, *2*, 2347.
[10] V. K. S. Hsiao, Y. B. Zheng, B. K. Juluri, T. J. Huang, *Adv Mater.* **2008**, *20*, 3528–3532.
[11] P. R. Evans, G. A. Wurtz, W. R. Hendren, R. Atkinson, W. Dickson, A. V. Zayats, R. J. Pollard, *Appl. Phys. Lett.* **2007**, *91*, 043101.
[12] a) Y. R. Leorux, J. C. Lacroix, K. I. Chane-Ching, C. Fave, N. Felidj, G. Levi, J. Aubard, J. R. Krenn, A. Hohenau, *J. Am. Chem. Soc.* **2005**, *127*, 16022; b) Y. Leroux, J. C. Lacroix, C. Fave, G. Trippe, N. Felidj, J. Aubard, A. Hohenau, J. R. Krenn, *ACS Nano* **2008**, *2*, 728; c) Y. Leroux, J. C. Lacroix, C. Fave, V. Stockhausen, N. Felidj, J. Grand, A. Hohenau, J. R. Krenn, *Nano Lett.* **2009**, *9*, 2144; d) V. Stockhausen, P. Martin, J. Ghilane, Y. Leroux, H. Randriamahazaka, J. Grand, N. Felidj, J. C. Lacroix, *J. Am. Chem. Soc.* **2010**, *132*, 10224.
[13] J. Dintinger, S. Klein, T. W. Ebbesen, *Adv. Mater.* **2006**, *18*, 1267.
[14] T. W. Ebbesen, H. J. Lezec, H. F. Ghaemi, T. Thio, P. A. Wolff, *Nature* **1998**, *391*, 667.
[15] H. Liu, P. Lalanne, *Nature* **2008**, *452*, 728.
[16] U. Schröter; D. Heitmann, *Phys. Rev. B* **1998**, *58*, 15419.
[17] B. K. Singh, A. C. Hillier, *Anal. Chem.* **2008**, *80*, 3803.
[18] B. K. Singh, A. C. Hillier, *Anal. Chem.* **2006**, *78*, 2009.
[19] B. Kaplan, H. Guner, O. Senlik, K. Gurel, M. Bayindir, A. Dana, *Plasmonics* **2009**, *4*, 237.
[20] A. Baba, K. Kanda, T. Ohno, Y. Ohdaira, K. Shinbo, K. Kato, F. Kaneko, *Jpn. J. Appl. Phys.* **2010**, *49*, 01AE02.
[21] a) A. Baba, N. Aoki, K. Shinbo, K. Kato, F. Kaneko, *ACS Appl. Mater. Interfaces* **2011**, *3*, 2080; b) A. Baba, K. Wakatsuki, K. Shinbo, K. Kato, F. Kaneko, *J. Mater. Chem.* **2011**, *21*, 16436.
[22] S. Mu, C. Chen, J. Wang, *Synth. Met.* **1997**, *88*, 249.
[23] W. S. Huang, B. D. Humphrey, A. G. MacDiarmid, *J. Chem. Soc. Faraday Trans.* **1986**, *1*, 82.
[24] J. C. Lacroix, K. Kanazawa, A. Diaz, *J. Electrochem. Soc.* **1989**, *136*, 1308.
[25] A. Baba, T. Mannen, Y. Ohdaira, K. Shinbo, K. Kato, F. Kaneko, N. Fukuda, H. Ushijima, *Langmuir* **2010**, *26*, 18476.
[26] L. A. A. Pettersson, F. Carlsson, O. Inganäs, H. Arwin, *Thin Solid Films* **1998**, *313–314*, 356.
[27] L. Groenendaal, F. Jonas, D. Freitag, H. Pielartzik, J. R. Reynolds, *Adv. Mater.* **2000**, *12*, 481.
[28] G. Sheppard, T. Oseki, A. Baba, D. Patton, F. Kaneko, L. Mao, J. Locklin, *Biomicrofluidics* **2011**, *5*, 026501.